

Plasmonic nanofocusing using a metal-coated axicon prism

Keisuke Kato,¹ Atsushi Ono,^{2,3} Wataru Inami,^{2,3}
and Yoshimasa Kawata^{1,3,*}

¹Department of Mechanical Engineering, Shizuoka University
3-5-1, Johoku, Naka, Hamamatsu 432-8581, Japan

²Division of Global Research Leaders, Shizuoka University
3-5-1, Johoku, Naka, Hamamatsu 432-8561, Japan

³CREST, Japan Science and Technology Agency, Japan

*kawata@eng.shizuoka.ac.jp

Abstract: We propose an excitation method for the localization of photons at the apex of a metal coated axicon prism. The cone angle of the prism and the metallic film thickness are designed to match the excitation conditions for surface plasmons. The plasmons propagate along the sides of the prism and converge at its apex. The resulting nanofocusing was investigated by simulating the intensity distributions around the apex of the prism using a finite-difference time-domain algorithm. For incident radial polarization, a localized and field enhanced spot is generated by the constructive interference of surface plasmons.

©2010 Optical Society of America

OCIS codes: (250.5403) Plasmonics; (240.6680) Surface plasmons; (180.4243) Near-field microscopy; (230.5440) Polarization-selective devices.

References and links

1. U. Kreibig and M. Vollmer, *Optical Properties of Metal Clusters* (Springer-Verlag, Berlin, 1995).
2. Y. Inouye and S. Kawata, "Near-field scanning optical microscope with a metallic probe tip," *Opt. Lett.* **19**, 159-161 (1994).
3. N. Hayazawa, Y. Inouye, Z. Sekkat, S. Kawata, "Near-field Raman imaging of organic molecules by an apertureless metallic probe scanning optical microscope," *J. Chem. Phys.* **117**, 1296-1301 (2002).
4. T. Ichimura, N. Hayazawa, M. Hashimoto, Y. Inouye, S. Kawata, "Tip-enhanced Coherent Anti-Stokes Raman Scattering for vibrational nanoimaging," *Phys. Rev. Lett.* **92**, 220801 (2004).
5. T. Okamoto and I. Yamaguchi, "Local plasmon sensor with gold colloid monolayers deposited upon glass substrates," *Opt. Lett.* **25**, 372-374 (2000).
6. P. Zijlstra, J. W. M. Chon, M. Gu, "Five-dimensional optical recording mediated by surface plasmons in gold nanorods," *Nature* **459**, 410-413 (2009).
7. W. Srituravanich, N. Fang, C. Sun, Q. Luo, X. Zhang, "Plasmonic nanolithography," *Nano Lett.* **4**, 1085-1088 (2004).
8. A. F. Koenderink, J. V. Hernandez, F. Roblcheaux, L. D. Noordam, A. Polman, "Programmable nanolithography with plasmon nanoparticle arrays," *Nano Lett.* **7**, 745-749 (2007).
9. E. Kretschmann and H. Raether, "Radiative decay of non-radiative surface plasmons excited by light," *Z. Naturforsch A* **23**, 2135-2136 (1968).
10. M. I. Stockman, "Nanofocusing of optical energy in tapered plasmonic waveguides," *Phys. Rev. Lett.* **93**, 137404 (2004).
11. W. Ding, S. R. Andrews, S. A. Maier, "Internal excitation and superfocusing of surface plasmon polaritons on a silver-coated optical fiber tip," *Phys. Rev. A* **75**, 063822 (2007).
12. N. A. Issa and R. Guckenberger, "Optical nanofocusing on tapered metallic waveguides," *Plasmonics* **2**, 31-37 (2007).
13. N. A. Janunts, K. S. Baghdasaryan, Kh. V. Nerkararyan, B. Hecht, "Excitation and superfocusing of surface plasmon polaritons on a silver-coated optical fiber tip," *Opt. Commun.* **253**, 118-124 (2005).
14. A. E. Babayan and Kh. V. Nerkararyan, "The strong localization of surface plasmon polariton on a metal-coated tip of optical fiber," *Ultramicrosc.* **107**, 1136-1140 (2007).

15. A. Bouhelier, J. Renger, M. R. Beversluis, L. Novotny, "Plasmon-coupled tip-enhanced near-field optical microscopy," *J. Microsc.* **210**, 220-224 (2002).
 16. H. Kano and W. Knoll, "Locally excited surface-plasmon-polaritons for thickness measurement of LBK films," *Opt. Commun.* **153**, 235-239 (1998).
 17. K. Watanabe, G. Terakado, H. Kano, "Localized surface plasmon microscope with an illumination system employing a radially polarized zeroth-order Bessel beam," *Opt. Lett.* **34**, 1180-1182 (2009).
 18. H. J. Lezec, A. Degiron, E. Devaux, R. A. Linke, L. Martin-Moreno, F. J. Garcia-Vidal, T. W. Ebbesen, "Beaming Light from a Subwavelength Aperture," *SCIENCE* **297**, 820-822 (2002).
 19. G. M. Lerman, A. Yanai, U. Levy, "Demonstration of Nanofocusing by the use of Plasmonic Lens Illuminated with Radially Polarized Light," *Nano Lett.* **9**, 2139-2143 (2009).
 20. W. Wolfe, *Handbook of Optics*, 2nd ed. (McGraw-Hill, New York, 1978).
 21. A. Taflov, and S. C. Hagness, *Computational Electrodynamics: The Finite-Difference Time-Domain Method*, 3rd ed. (Artech House, Norwood, 2005).
-

1. Introduction

The localization of photons by local surface plasmon resonance (LSPR) is quite attractive for researchers as an approach to break through the diffraction limit of light [1]. It was proposed that a metallic probe tip localized photons at the tip apex by LSPR [2]. They have then been used as a nanometric light source for near-field scanning optical microscopy [3, 4]. A gold colloidal monolayer has been employed as an optical sensor because LSPR is sensitive to the thickness and the refractive index of the medium surrounding the nanoparticles [5]. Five-dimensional optical recording has been demonstrated based on the spectral and polarization properties of LSPR in recording media [6]. Plasmonic nanolithography has recently been developing with the experimental demonstration of 90 nm dot array patterns by silver nanoholes [7], along with calculations of distinct patterns from a single lithographic mask of silver nanoparticles [8]. The LSPR is enhanced at the vicinity of the metallic nanoparticles and there is no need for the momentum adjustment which makes the LSPR of nanoparticles easily excitable by propagating waves, but the efficiency of the excitation of LSPRs on metal nanoparticles is limited even with tight focusing because the size of the nanoparticles is still much smaller than the focal spot.

Recently, many researches have been reported that light is plasmonically focused to nanoscale by the surface plasmons traveling metallic tip [9-13]. Novotny's group has proposed that a local excitation source is created by the initial waveguiding of radially polarized light in the metal-coated fiber tip; that source was used for near-field optical microscopy [14]. A nanofocused spot was generated by constructive interference of SPRs on the coaxial structure of metal surfaces or films irradiated with tightly focused radially polarized light [15-17]. Lezec et al. have shown that beaming of enhanced light transmission emerges from a nano-aperture in the groove structure of silver [18]. The groove structure at the exit side modifies the radiation pattern.

In this letter, we propose a LSPR light-harvesting method of converting the propagation mode of a surface plasmon resonance (SPR) into an LSPR via the Kretschmann configuration [19]. However, the efficiency of the excitation of LSPRs on metal nanoparticles is not high even with tight focusing because the size of the nanoparticles is still much smaller than the focal spot.

2. FDTD simulation

Figure 1(a) shows the proposed structure of our metal-coated axicon prism. It generates an enhanced spot at the apex by the localization of SPRs excited on the side surface of the axicon in the Kretschmann configuration. The SPRs are excited with a high coupling efficiency and are subsequently converted into LSPRs at the apex. The excitation mechanism and the localization of photons by the axicon prism are investigated using a finite-difference time-domain (FDTD) simulation. Figure 1(b) shows the design used for this purpose. The SPRs are excited at an incident wavelength of 632.8 nm in the gold of permittivity $10.97+1.35i$ [20]. The optimal thickness of the gold and the excitation angle in the Kretschmann configuration

are 47.5 nm and 44.0 degrees, respectively. Therefore, the half-cone angle is determined as 46.0 degree. The radius of curvature of the apex of the prism is designed to 25 nm.

In the FDTD simulation, an adaptive mesh with grid sizes that vary between 1 and 10 nm is used to investigate the optical dynamics at the apex, while ensuring the calculations can be handled by the memory of the computer. A volume of $50 \times 50 \times 60 \text{ nm}^3$ represents the prism apex at the smallest grid size of 1 nm. The calculations extend over $2.4 \times 2.4 \times 1.4 \mu\text{m}^3$. A perfectly matched layer is assumed for the boundary conditions [21]. The mechanism of the plasmonic nanofocusing by the gold-coated axicon prism are investigated for radial, azimuthal, and linear optical polarizations. The enhancement and the spot size at the apex are also studied.

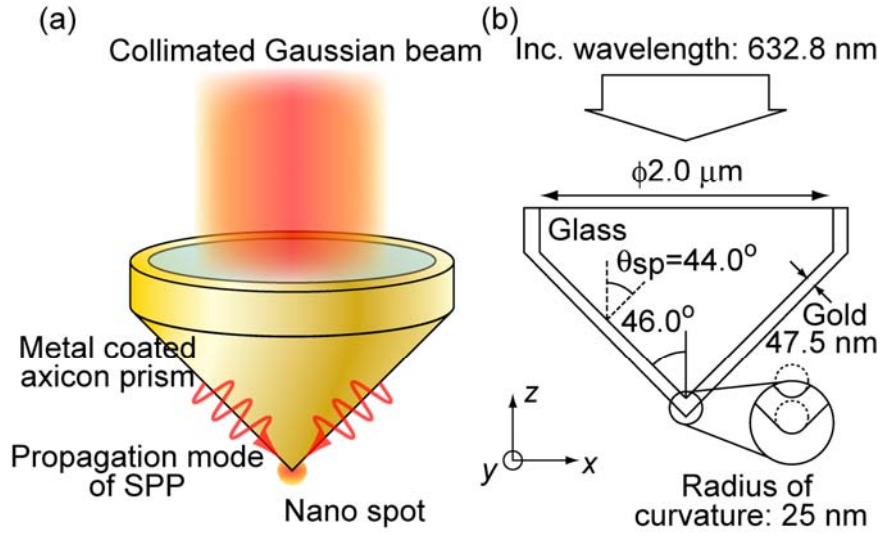


Fig. 1. (a) Schematic for the localization of photons by a metal-coated axicon prism. A collimated Gaussian beam is incident on the prism and surface plasmons are excited along the sides. A nano spot is generated at the apex by constructive interference of surface plasmons. (b) Model of the device as simulated by an FDTD algorithm, for He-Ne laser excitation at a wavelength of 632.8 nm. A gold coating is used because of its chemical stability. The curvature at the apex corresponds to a diameter of 25 nm. The film thickness of gold and the half cone angle of axicon prism are determined to be mostly excited surface plasmons by normal incidence to the top surface of the prism.

3. Results and discussion

The intensity distribution at a vertical (x - z) cross section of the prism when a simulated Gaussian beam with radial polarization is incident on the prism is shown in Fig. 2(a). Enhanced intensity is observed on the side of the prism and at the apex. All of the surface plasmons excited on the side are found to propagate in phase and constructively interfere at the apex. Despite radial polarization incidence which has non-zero electric field at the center, we see the strong intensity at the center inside the prism. This is because the reflection from the all direction of side surface in three-dimension is constructively interfered at the center.

Figure 2(b) presents a magnified view of the apex. A bright spot can be seen there. Figure 2(c) is the intensity distribution at a lateral (x - y) cross section 5 nm below the apex. The intensity profile across the center a - a' in Fig. 2(c) is plotted in panel (d). The spot has a full-width-at-half-maximum of 35 nm and a peak intensity that is 1.2×10^2 times larger than at the apex.

The electric field is the most enhanced at the just below the apex, and the field exponentially decays with the distance. In these simulations, we meshed the size with 1 nm, therefore the field at 1 nm below the apex exhibits the most high intensity. However, we have applied 5 nm away from the apex due to the following reasons. (●) In the FDTD simulation,

we see the unfavorable spikes in the spot where the plane at 0 -4 nm below the apex because of the strong fields are shown at the corner location of the apex which is caused by the simulation area is meshed with 1 nm grid. Gaussian spot is obtained at planes more than 5 nm away from the apex. (□) Considering the applications of this technique to microscopy, we need a few nanometers distance between sample and the apex, so we assume the distance is 5nm.

Note that the monochrome scales are different in Figs. 2(a) and 2(b). The scale in Fig. 2(a) has a peak saturation value of 5 to show the propagation mode of SPRs excited on the side surface. On the other hand, the scale in Fig. 2(b) has a peak saturation value of 50 to show the localization of photons at the apex.

We measured the polarization components of the electric field of the LSPRs for incident radial polarization. Figure 3(a) shows that the E_x component is enhanced near the apex of the prism but disappears at its exact center, whereas Fig. 3(b) shows that the E_z field is maximized at the center. Furthermore, the E_z peak intensity is 10 times higher than that of E_x . Thus the z -polarized component is dominant. The incident light has both E_x and E_y components but they are converted to an evanescent field with an E_z component, due to the excitation of surface plasmons.

We also investigated the intensity distributions for incident linear and azimuthal polarizations to understand the mechanisms of the excitation and localization of SPRs. Figure 4(a) shows the electric field distribution in a vertical cross section including the central prism axis for linearly polarized illumination. In this case, SPRs are excited on the sides of the axicon as radial polarization, but the spot is not localized at the apex. The inset of Fig. 4(a) shows the intensity distribution for a lateral cross section 5 nm below the apex. The line profile is the intensity distribution along the dashed line in the figure. In the case of azimuthally polarized excitation, SPRs are not excited and so there is no localization at the apex as shown in Fig. 4(b). Thus, the nature of the incident polarization significantly affects the excitation of LSPRs at the apex.

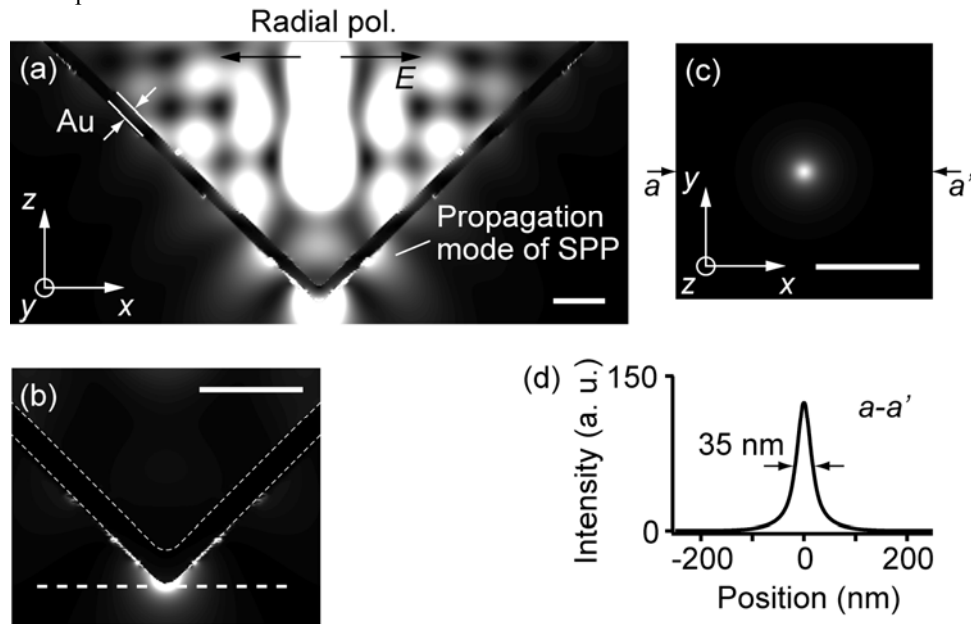


Fig. 2. Intensity distributions on a gold-coated axicon prism for radially polarized incident light. (a) A vertical (x - z) cross section including the central axis of the prism. Field enhancements are observed on the side surface due to excitations of surface plasmons. (b) Enlarged image showing a hot spot generated at the apex. (c) A horizontal (x - y) cross section 5 nm below the apex, corresponding to the dashed line in (b). (d) Intensity profile along line a - a' in (c). The FWHM of 35 nm is obtained. The scale bar in each figure is 200 nm long.

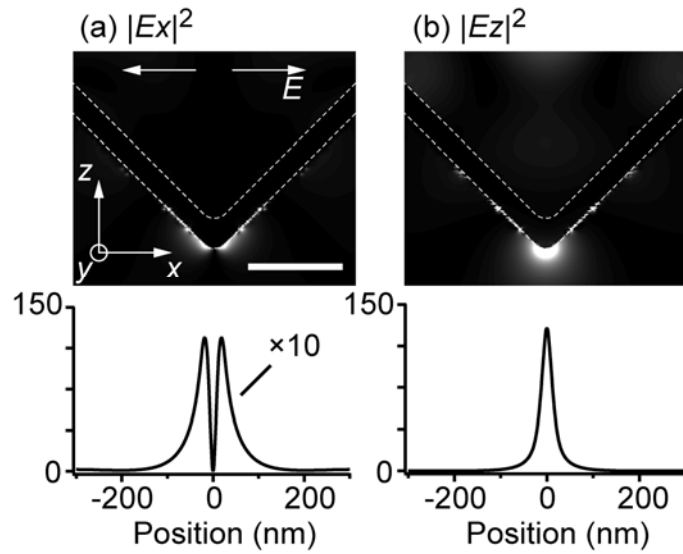


Fig. 3. Localization of photons for incident radial polarization for electric field component (a) E_x and (b) E_z . The upper figures show vertical cross sections of the intensity distributions of the electric field components. The lower figures plot profiles 5 nm below the apex, just as in Fig. 2. The E_x component near the apex bifurcates in two and is magnified 10 fold in the graph. The E_z component is maximized at the apex. The scale bar in the first photograph is 200 nm long.

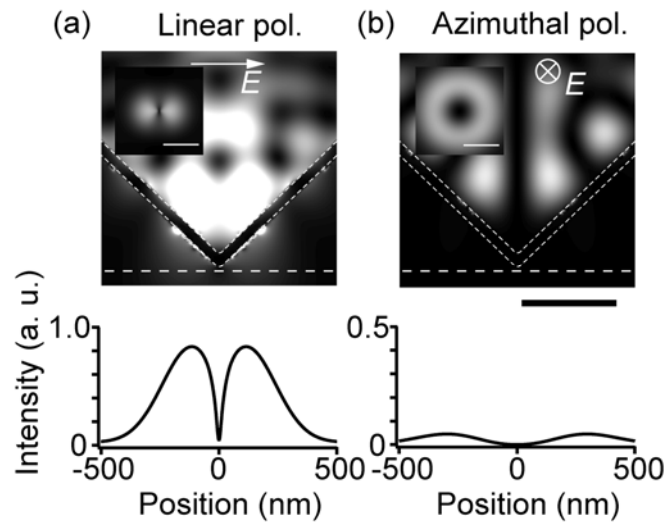


Fig. 4. Intensity distributions for incident (a) linear and (b) azimuthal polarizations. The insets show horizontal (x - y) cross sections of the intensity. The lower profiles plot the intensity along the dashed line located 5 nm below the apex. (a) Although enhanced fields are observed on the side surfaces for linear polarization, an enhanced spot is not observed at the apex. The surface plasmon is canceled by destructive interference there. (b) The fields on the surface are very small for incident s-polarization. The scale bars in the photographs are 400 nm long.

We conclude that the confined hot spot at the apex is generated by the conversion of LSPRs from SPRs excited by the Kretschmann configuration at the side surface. The combination of the radial polarization and the cone shape of the prism is necessary to excite

SPRs, which propagate and are focused onto the apex. Then the enhanced spot is localized at the apex by the constructive interference of the focused SPRs.

In the FDTD simulations, the thickness of the gold film and the half-cone angle of the axicon prism are optimized for the incidence of collimated light to excite SPRs. There is some uncertainty in the optimum 47.5-nm value of the thickness due to the 10-nm grid size (limited by the computer memory), as shown in Fig. 5(a). (Note however that the volume around the apex uses a fine 1-nm grid mesh, in order to accurately evaluate the localization of SPRs.)

Figure 5(b) shows the reflectance in the Kretschmann configuration as a function of the incident angle for various thicknesses of gold film near the optimum value. The reflectance has a minimum at an incident angle of 44.0 degrees for a thickness of 47.5 nm. So those values are the best coupling conditions for SPR excitation at a wavelength of 632.8 nm. The excitation efficiency decreases by about 10% at 40 and 60 nm thicknesses. The grid size affects not only the thickness but also the roughness of the surface. In our simulations, a 1.2×10^2 field enhancement is obtained for incident radial polarization (with an uncertainty of less than 10%) and it is expected to be further enhanced if a finer mesh size is used.

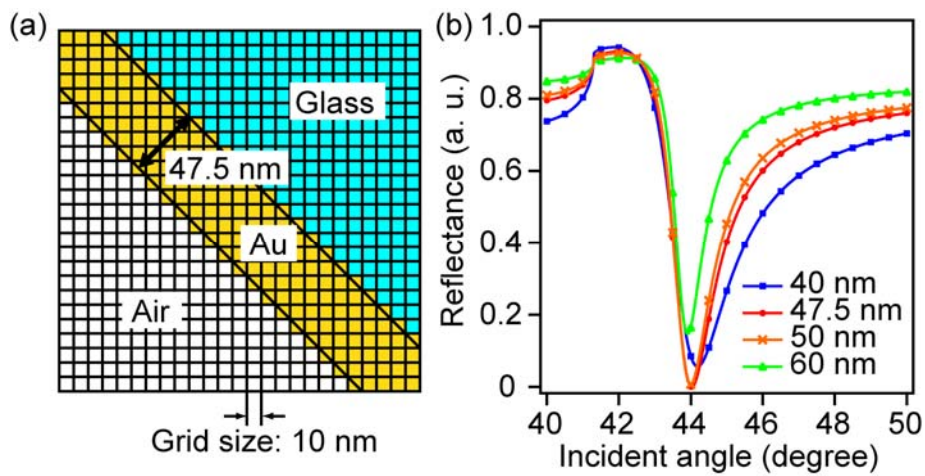


Fig. 5. Simulation uncertainty due to the grid size in the FDTD calculations. (a) Schematic of a computer aided design on the side surface of an axicon prism. Each grid has a side of length 10 nm. The gold thickness is between 40 and 60 nm. (b) Numerical calculations of the reflectivity as a function of the incident angle and thickness in the Kretschmann configuration. The reflectance decreases at an incident angle of 44 degrees. The incident light couples with surface plasmons at this angle.

4. Conclusion

We have proposed an efficient LSPR excitation method for the localization of photons beyond the diffraction limit by converting the propagation mode of SPRs to LSPRs by using a gold-coated axicon prism. Radially polarized incident light excites SPRs at the surface of the prism and generates an enhanced spot confined within 35 nm of the apex for an incident wavelength of 632.8 nm. The Kretschmann configuration of the axicon is efficient for light harvesting excitation. The spot generated from a collimated Gaussian beam without use of a lens could be utilized as a nanometric light source for optical imaging, optical memory, and laser fabrication with nanoresolution.